Maximizing the Power Output of a Solar Photovoltaic Panel Using Fresnel lens Concentrator

Alexander A. Willoughby[1,2], Ayodele O. Soge[1], Oluropo F. Dairo[3], Ruth Asi[4]

[1]Department of Physical Sciences, Faculty of Natural Sciences, Redeemer's University, PMB 230, Ede, 232102, Osun State, Nigeria

[2]Centre for Alternative Technology, University of East London, Machynlleth, Wales, SY20 9AZ, United Kingdom

[3]Department of Electrical and Electronic Engineering, Faculty of Engineering, Redeemer's University, PMB 230, Ede, 232102, Osun State, Nigeria

[4]Department of Electrical and Electronic Engineering, Faculty of Engineering, University of Calabar, PMB 1115, Etagbor, 540271, Cross-River State, Nigeria

DOI: https://doi.org/10.51584/IJRIAS.2025.100600132

Received: 14 May 2025; Accepted: 21 May 2025; Published: 22 July 2025

ABSTRACT

This paper reports the performance of a solar photovoltaic module subjected to increased radiation from a Fresnel lens in a low concentration system. An experimental, comparative investigation of two photovoltaic modules was carried out. The test module was subjected to concentrated radiation from the Fresnel lens while the control module was directly exposed to the sun. Current-voltage characteristics of both modules were measured for different days and irradiance conditions. Module temperature and variations of irradiation received were equally measured. The results obtained confirmed that the short circuit current and the maximum power output of the test module were higher than those of the control module. This trend was observed for different levels of insolation ranging from ~158 W/m^2 to ~1070 W/m^2. The test module displayed an average increase in short circuit current of over 41% than that of the control module. Additionally, the test module with concentrated solar radiation from the Fresnel lens could produce between 32% and 56% more current at maximum power than the control module, depending on the amount of insolation received. The concept demonstrated in this study has a potential application in rapid battery charging during low solar irradiation and other functional applications where twice as much energy is needed in a short duration.

Keywords: Solar photovoltaic panel, Concentrated photovoltaic, Fresnel lens concentrator, Solar energy, Irradiation, Maximum power point

INTRODUCTION

For several decades now, it has been a recognized reality that the consumption of energy from conventional energy sources, such as the burning of fossil fuel for convenience and subsistence, has impacted negatively on the climate and environment. Greenhouse gases (GHGs), climate change, and global warming are a few expressions applied in academic and political discourse to describe the ensuing environmental degradation [1]. Awareness, followed by apprehension at the diminishing stock of traditional fossil fuels and the attendant problem of atmospheric pollution, has led to an affirmative drive towards the exploitation of solar photovoltaic energy as one of the renewable energy alternatives. The sun provides the Earth with constant energy in the form of heat, light, and radiation. Electricity can be generated from solar energy either by photovoltaic (PV) or

ISSN No. 2454-6194 | DOI: 10.51584/IJRIAS |Volume X Issue VI June 2025

solar thermal technologies [2]. The exploitation of solar resources in the implementation of solar PV systems has the advantage that no fuel or fuel supply chain is required. Its main fuel is the photons reaching the earth from the sun. PV electricity offers a practicable alternative to fossil fuels in that it does not involve the depletion of natural resources of coal and oil. Thus, solar energy is a renewable source of electricity generation. The generation of electricity from PV does not involve the emission of air contaminants, i.e., zero-level pollution, although toxic chemicals are used and modest quantities of hazardous emissions are produced in the PV manufacturing process wherein silica extraction involves fossil fuels [2] [3]. Another source of concern that may ensue regarding the environmental impact of PV electricity generation is the land surface area per megawatt of capacity required and the effects on ecosystems. Building integrated PV (BIPV) installations, where PVs are installed on building roofs or facades can eliminate land space taken up by PV installations [4].

Solar PV technology has come a long way since its invention. Its developmental process has been dogged by issues such as low conversion efficiency on the back of the high cost of investment and production [2]. Over the years, its progress has dramatically improved by developing innovative and progressive technologies. Under laboratory test conditions, an efficiency of 24% from the best single junction silicon solar cells has been attained, while efficiencies of over 17% have been produced for crystalline PV modules [2]. So far, 13-14% cell conversion efficiency has been achieved for commercially mass-produced solar cells [5] [6], although a 20% conversion efficiency can be achieved. Efforts are still being made to improve conversion efficiencies towards the presently acknowledged theoretical 30% limit. Even with these improvements, researchers are ever in pursuit of ways of maximizing the outputs of cells over the specifications of manufacture. Different methods can be utilized to maximize the output of PVs. Concepts such as maximum power point tracking (MPPT) [6] and concentrating photovoltaic (CPV) [7] allow increased outputs to be significantly obtained. The MPPT changes the equivalent array load by adjusting the working point of the array so that maximum power is attained as temperature and solar intensity vary [6]. Another method involves mirrors or lenses, which are used to concentrate incoming sunlight onto the PV cells [2]. The benefit of this is the utilization of small and high-efficiency PV cells such as compound (III-V) PV cells, with efficiency as high as 40% under concentration [8]. Due to the small spot size generated from a concentrator, the cell can be made as small as 1 cm2. These concentrating systems are equipped with sun trackers [5] which follow the path of the sun at zenith and azimuthal angles so that its rays are directly concentrated on the cell or module. They must also be cooled to prevent overheating of the cells [9]. The elevated PV surface temperature constitutes a major problem for CPV which can be solved using a Concentrating Photovoltaic Thermal (CPVT) system as reported by [10]. The proposed hybrid system comprising CPV and the solar thermal system was based on Point Focus Fresnel Lens and embedded Multi Junction Photovoltaic (GaInP/InGaAs/Ge) cells. The experimental results showed that the CPVT system delivered the highest thermal and electrical efficiencies of 49.5% and 36.5%, respectively. Hence, the proposed system has vast potential to compete with conventional power generation systems. According to [9] [11], CPV Fresnel concentrators are becoming attractive amongst non-concentrating systems as the price of mirrors and Fresnel components is dropping. Besides, the CPV Fresnel concentrators could be considered a good alternative in the case of the rising cost of PV panels.

Furthermore, it has been reported that the integration of compound parabolic concentrator (CPC) and phase change materials (PCMs) in photovoltaic/thermal (PV/T) systems is an effective method for improving electrical and thermal performance simultaneously [12]. The thermal and electrical performance of a compound parabolic concentrating PV/T system combined with PCM (PV/T-CPCM) was experimentally analysed in an outdoor environment by Kong et al. [10]. The experimental results revealed that the temperature non-uniformity factor of PV modules/PCM sharply decreased from 4.28/1.34 to 1.42/0.66 as the PCM melted from solid to mushy state due to variations in temperature and solar irradiance during the test period. This outcome depicts that the PCM enhanced the non-uniformity of temperature distribution. Additionally, the PV/T-CPCM system produced a higher maximum primary energy efficiency of ~ 7.9% and 10.7% compared to that of the separate PV-CPC and PT-CPC systems, respectively, indicating that the PV/T-CPCM system possesses superior heat-electricity cogeneration performance [12].

Alzahrani et al. [13] demonstrated the use of graphene as a pre-illumination cooling approach for a CPV system. A screen-printed graphene coating (GC) was experimentally characterized to evaluate the light

ISSN No. 2454-6194 | DOI: 10.51584/IJRIAS |Volume X Issue VI June 2025

attenuation across a broad wavelength range with various GC thicknesses on a low-iron glass. The GC acting as a neutral density filter for the focal spot CPV system reduced the device temperature remarkably by 20% and 12% for GC6.3 (6.3 μm thickness) and GC2.2 (2.2 μm thickness) compared to the infrared filter, respectively. Thus, the GC thickness plays a critical role in the overall performance of the CPV system. Also, the cell efficiency of the CPV system was increased by GC6.3 by ~12% at 8 suns in comparison with the base case at 400 W/m^2, producing 7 suns. This increase in cell efficiency is attributed to the excellent thermal filtering of graphene.

Guiqiang et al. [14] investigated the effects of different finger numbers and spacing on the electrical performance of low-concentrating photovoltaic cells (LCPVs) using the non-uniform illumination distribution formed by the concentrator. Experimental results showed an increase in the efficiency of the LCPV from 13.805% to 13.837% due to the optimization of the numbers and spacing of the front metal fingers in the crystalline silicon solar cell. This finger optimization technique implemented by the authors is an effective approach in enhancing the efficiency of CPV cells. In regions where there are lots of diffuse radiations, some alternative designs of concentrator systems permit both direct and diffuse radiation to be concentrated [2]. For instance, [8] investigated the effect of diffuse radiation on a Fresnel-based CPV system using a secondary optical element (SOE) made of flat plate reflectors. The proposed CPV system with SOE exhibited at least 10% higher efficiency than the conventional CPV system without SOE. As the diffuse radiation ratios increased from 0.1 to 0.4, the proposed system efficiency increased from 11 to 23%. Besides, a 20% higher energy gain was delivered by the proposed CPV system than the conventional CPV system.

In developing countries, particularly in sub-Saharan Africa, reliance is mainly on four sources of energy, viz: imported petroleum fuels, biofuels, hydroelectric, and geothermal power [15]. For instance, in Nigeria, the high cost of PVs is beyond the means of the general population, especially those living in rural communities who are not connected to the electricity grid. For those connected to the grid in the urban areas, the unstable and epileptic nature of the distributed power makes it almost impossible to conduct businesses requiring electricity. The stand-alone photovoltaic systems with the lead-acid battery as energy storage hold great potential for developing countries in accessing affordable and clean energy in tandem with the 7th UN's Sustainable Development Goal. However, meeting the cost of the sized estimate of components of a system to match the load requirements is difficult, and the prospective solar PV system owner may be forced to downsize the whole system, in most cases by reducing the number of modules and hence compromising power output. To overcome this challenge, the number of panels estimated from dedicated PV sizing software or simple calculations can be reduced by increasing the output current of the PV itself using concentrator methods.

This study aims to investigate the viability of implementing a concentration system using a Fresnel lens on a monocrystalline PV module to increase the power output at a fraction of the actual cost, through increased light concentration rather than buying additional modules to meet the power estimates of a particular load.

MATERIALS AND METHODS

Proposed CPV System

A comparison between the proposed method and a conventional system is demonstrated in Fig. 1. The proposed CPV system is both unconventional and different from the conventional CPV system using III-V semiconductors. It is designed to be a low-concentration system in which the lens is positioned over the PV module such that its focal spot does not converge onto the module but behind it. Thus, no active cooling is required by the proposed CPV system since it does not suffer from elevated PV surface temperature.

Fresnel Lens and Module Positioning

Two PV modules of the same characteristics (Appendix 1) were used for the experiment. The test module had a Fresnel lens placed over and above it, while the control module was directly exposed to sunlight.

ISSN No. 2454-6194 | DOI: 10.51584/IJRIAS |Volume X Issue VI June 2025

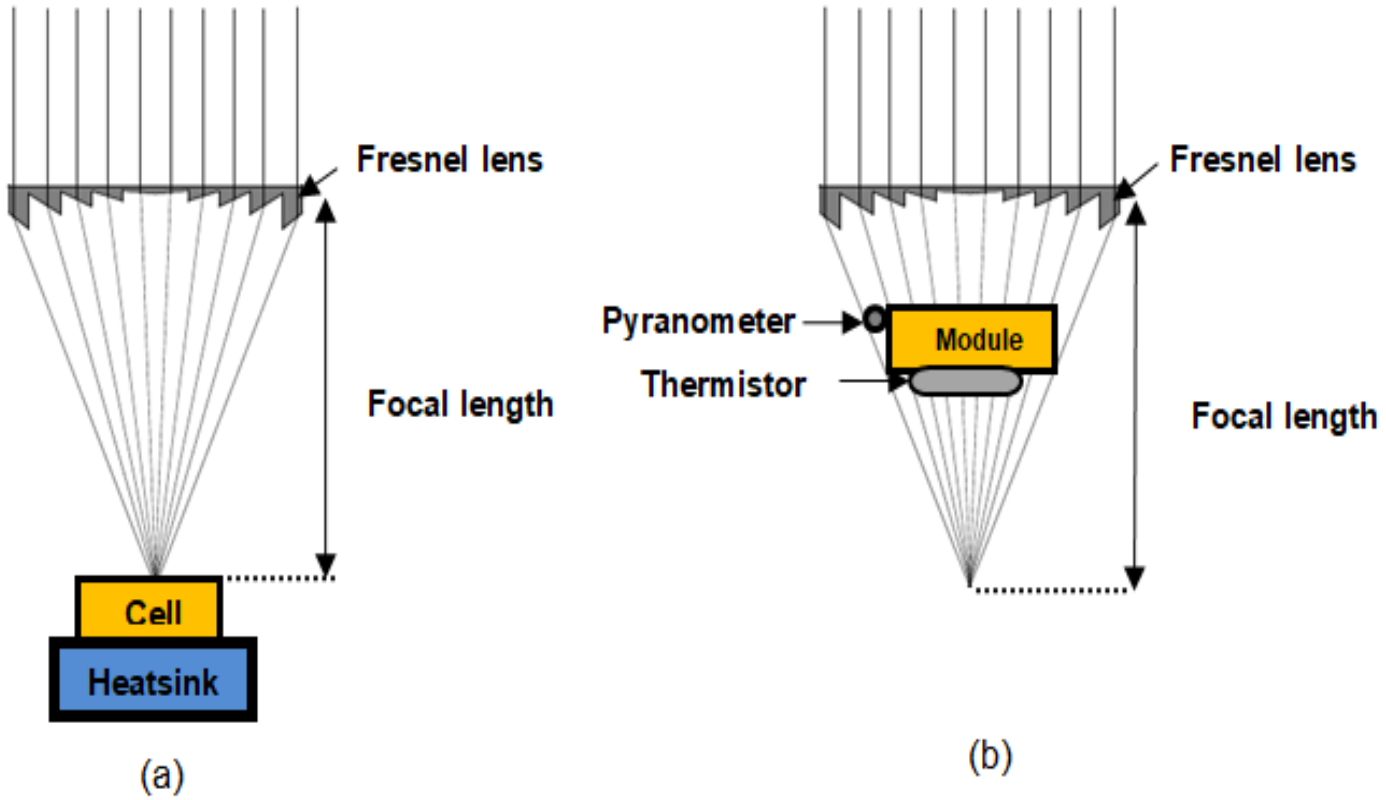

Fig.1. (a) Conventional solar cell Fresnel concentrator and (b) proposed concept.

Fig. 2 shows the schematic diagram of the experimental setup featuring the relative positions of the lens, modules, and sensors. Each module is 130 mm x 130 mm in size, and both modules were fixed approximately 1cm above a flat particle board with approximately 50 cm separation between the two. The Fresnel lens was first framed with light wood. The frame was then positioned directly above the test module, with its centre in alignment. Four supporting bolts and nuts were used to hold the frame above the module. The distance between the lens and the module, *h*, was made adjustable so that lens-module separation could be varied. By varying the lens-module distance, a compromise distance of about H = 2.5 cm separation between the lens and module was found to be most suitable for the beam to cover both the lens and the irradiation sensor placed beside it. By increasing the distance, the beam from the lens would not envelop both the module and the pyranometer, and no significant voltage and current would be generated. Since the experiment was considered a low concentration type, a sun tracker was not deployed, and the setup was simply of a static type aligned to face the sun. As the sun's position changed, it was merely manually adjusted to follow the sun's path. It should be noted here that the performance of a solar module is improved with the implementation of solar tracking [16], either with a one-axis tracker which automatically follows the sun in an east-west path during the day or for better accuracy and enhanced capture, a two-axis type that tracks in both altitude and azimuth directions.

Data Collection Procedure

The assembly, consisting of the Fresnel lens, photovoltaic modules, and sensors, was carried outside on sunny days to different areas where there were no obstructions to the direct rays of the sun. The setup was mounted on a support and oriented to face the sun. A check was made to ensure that the image (beam) exiting the Fresnel lens covered the module and pyranometer. The experiment was conducted for several days between 14 November 2010 and 28 December 2010 under varying sunlight conditions. In-situ measurements of current, voltage, thermistor (temperature), and pyranometer (irradiation) readings were logged directly by the programmed Pace XR5 data logger. The location was in the southeast of London, SE11 5TR, coordinates Lat. 51˚ 28′N, Long.-0˚ 6′W. As the period of observation was during the winter, usually, the sun appeared between 0900 hrs and 1400 hrs before it disappeared behind either the clouds or the multi-story buildings. Most of the readings were therefore taken between 0900 and 1400 hrs. Whenever the position of the sun shifted, the assembly position was also moved to align with the sun before logging commenced.

ISSN No. 2454-6194 | DOI: 10.51584/IJRIAS |Volume X Issue VI June 2025

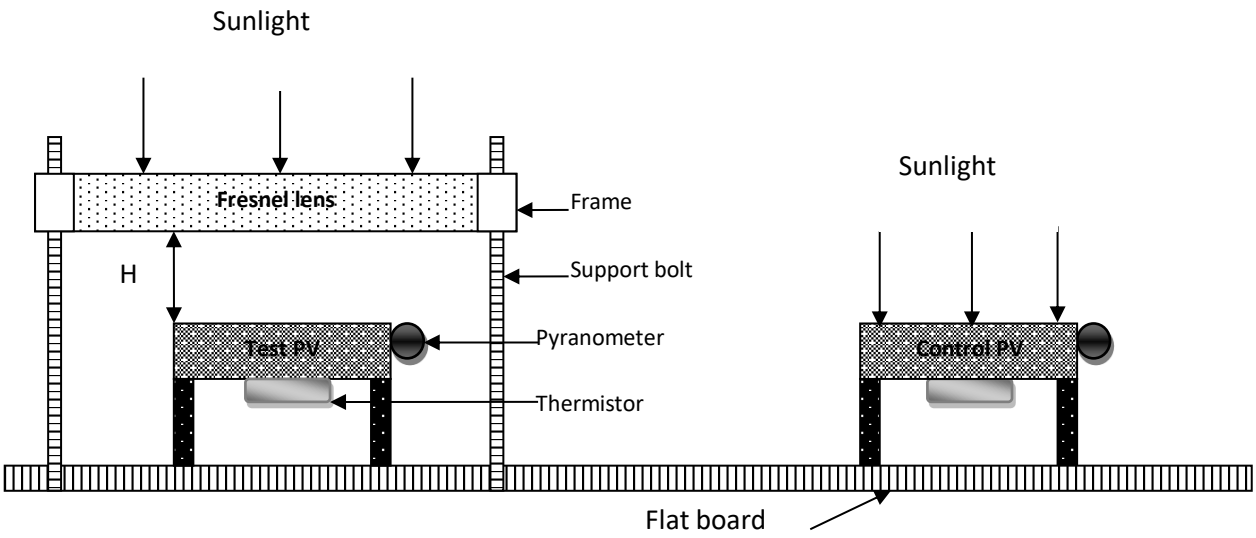

Fig. 2. Diagram of the setup comprising the Fresnel lens, modules, pyranometers, and temperature sensors

The photograph of the experimental set-up is shown in Fig. 3.

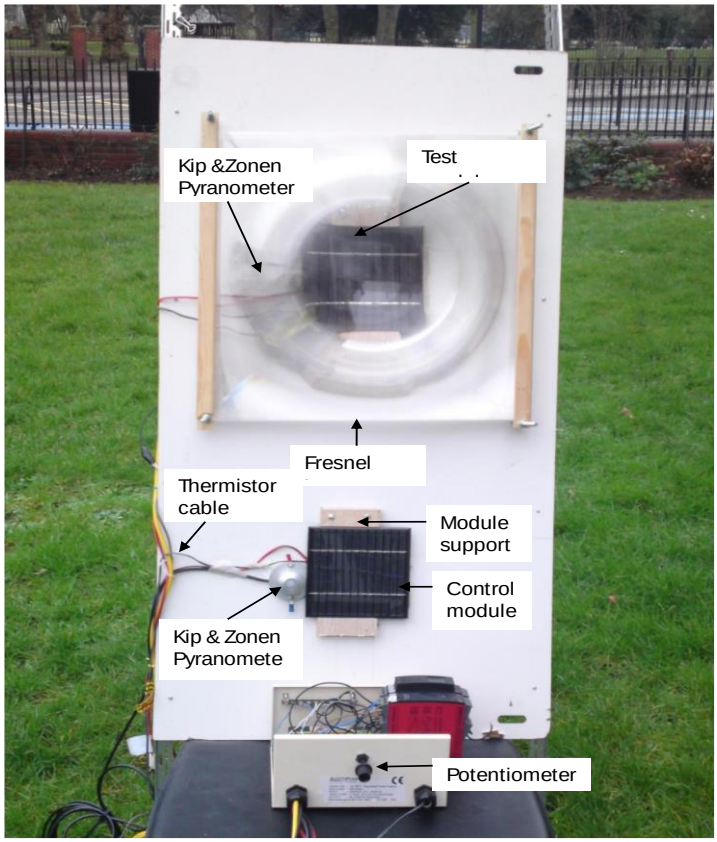

Fig. 3 Photograph of the assembly of the experimental setup

Measurements

Measurements of relevant data associated with performance characteristics of solar PVs were taken for both test and control modules.

1) *Current-Voltage Characteristics*:

The schematic of the side-by-side measurements of the voltages and currents of the test and control panels, respectively, is displayed in Fig. 4. Normally, the industry standard for measuring a solar cell output is to

ISSN No. 2454-6194 | DOI: 10.51584/IJRIAS |Volume X Issue VI June 2025

multiply the measured short circuit current and open circuit voltage to obtain the cell's rated power [17]. On the other hand, this procedure does not give the exact useable power output of the cell. Therefore, a switchable or varying load is preferable so that maximum power points under varying light conditions can be located. Solar radiation was allowed to fall on the modules and the short circuit current and voltage were measured by quickly varying the dual ganged 5 kΩ rheostat or potentiometer (pot'), VR, in series with a current meter (shunt resistance, RS) from zero to maximum and back. The purpose of the dual gang potentiometer is to ensure that both modules see the same load resistance at the same time as the pot' is being varied. The maximum power output obtainable from the module will occur when the load resistance corresponds to the operating point of the module. The following data were collected:

(i) I-V and P-V characteristics for control and test panels.

(ii) Irradiance at control panel and at test panel.

(iii) MPP of PV under various sunlight conditions by varying the resistive load, which is the ganged potentiometer and, deducing power.

(iv) Temperature of panels.

2) *Irradiation measurement*:

3) Each module had a Kip and Zonen pyranometer irradiance sensor (with a sensitivity of 71 μV/Wm^{-2}) attached to its edge and level with its surface. For the test module, the Fresnel lens was placed closely above it such that the concentrated beam, approximately 140 mm in diameter, emanating from it was allowed to spread over the whole area of the module, while also covering the pyranometer. Spot concentration on the module was avoided in this way, the lens' focus appearing well behind the module.

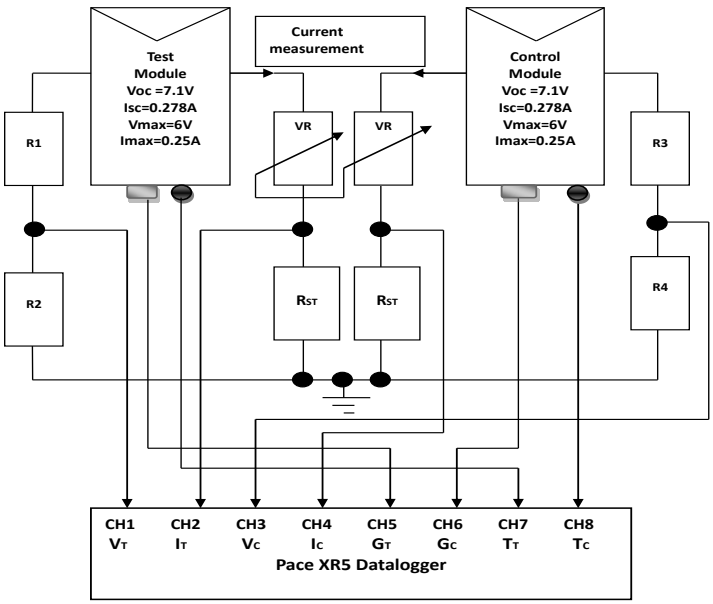

Logger Channel Designations:
CH1: Test module voltage, V_T; CH2: Test module current, I_T;
CH3: Control module voltage, V_C; CH4: Control module current, I_C;
CH5: Test module irradiance; G_T; CH6: Control module irradiance, G_C;
CH7: Test module temperature, T_T; CH8: Control module temperature, T_C.

Fig. 4. Schematic of the side-by-side in-situ current, voltage, irradiance, and temperature measurements.

3) *Temperature measurement*

A cylindrical-shaped thermistor temperature sensor was fitted into a cylindrical copper conductor and attached to the back of the test module. Another thermistor was positioned in close thermal contact with the control

ISSN No. 2454-6194 | DOI: 10.51584/IJRIAS |Volume X Issue VI June 2025

module to measure the ambient temperature. The corresponding leads from each sensor were connected to the configured inputs of the Pace XR5 datalogger (Fig. 5).

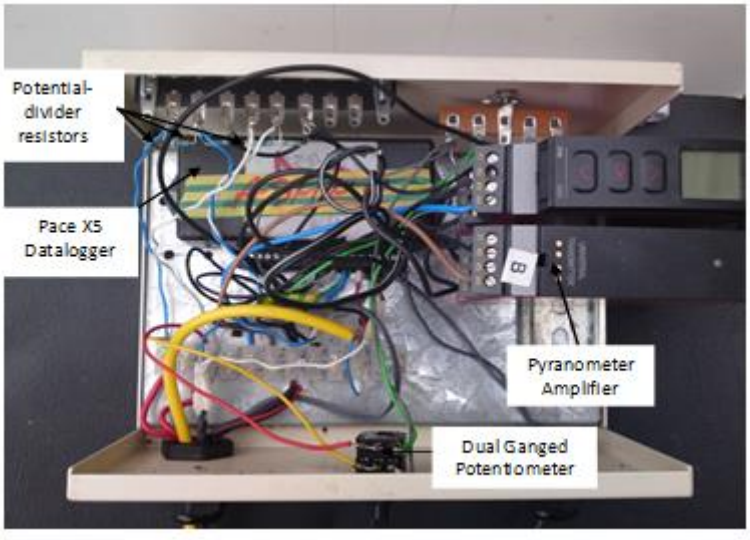

Fig. 5 Connections to the datalogger inputs

4) *Voltage and scaling current*: The maximum input voltage that the Pace XR5 datalogger can accommodate is 5V. Therefore, the module voltage was scaled down using potential dividers to a safe enough value for the signal input into the data logger. The current was measured by measuring the voltage across the shunt resistor RST and divided by its value. Data analysis was carried out by obtaining and plotting current-voltage (I-V) and power-voltage (P-V) characteristics of the modules for different insolation levels, from data downloaded from the data logger.

RESULTS AND DISCUSSION

A. Current-Voltage and Power-Voltage Characteristics

The Current-Voltage (I-V) and Power-Voltage (P-V) characteristics of the test and control panels were obtained for high, medium, low, and very low insolation days. The results obtained are presented in Fig. 6.

1) *Current-voltage characteristics*: For comparison, characteristic curves from both the test and control modules have been plotted on the same chart. It is evident from the curves that the increased light intensity generated because of improved concentration by the lens contributed to an increase in the short circuit current and maximum power point. The maximum power point, PMPP, is seen to have changed position and increased significantly due to the influence of the lens. Each point on the curve was determined by varying the 5 kΩ 'pot' load resistance from zero to maximum, measuring current and voltage. Somewhere along each I-V curve, the maximum power point (in watts-peak) was reached.

As shown in Fig. 6(a), on a high insolation day, the current at maximum power, IMPP, was found to increase by 41% from 0.190 A to 0.267 A. Similarly, on both medium and low insolation days, the I-V curves in Figs. 6(b) and (c) also show a percentage increase in IMPP of 32% and 56% for a corresponding increase of 20% and 39%, in irradiation, respectively. On a very low insolation day, 24 December 2010, as depicted in Fig. 6(d), there was a slight increase in ISC from 0.021 A to 0.055 A. It is interesting to note that the value of irradiation falling on the test module was lower at 158 W/m2 than that on the control module which was recorded as 172 W/m2. Also, the temperature of the test module remained higher at 9.6 ˚C than the control module which was at 4.3 ˚C. This condition may be attributed to attenuation or radiation transmission loss resulting from reduced solar energy incidents on the lens. The I-V curve for this day is almost linear-like as observed in Fig. 6 (a). Usually, near linear-like curves are suggestive of a large series resistance, RS, and shunt resistance Rsh of the module material that can affect the fill factor. The highest percentage increase of IMPP was observed to be approximately 64% for the duration of the experiment.

ISSN No. 2454-6194 | DOI: 10.51584/IJRIAS |Volume X Issue VI June 2025

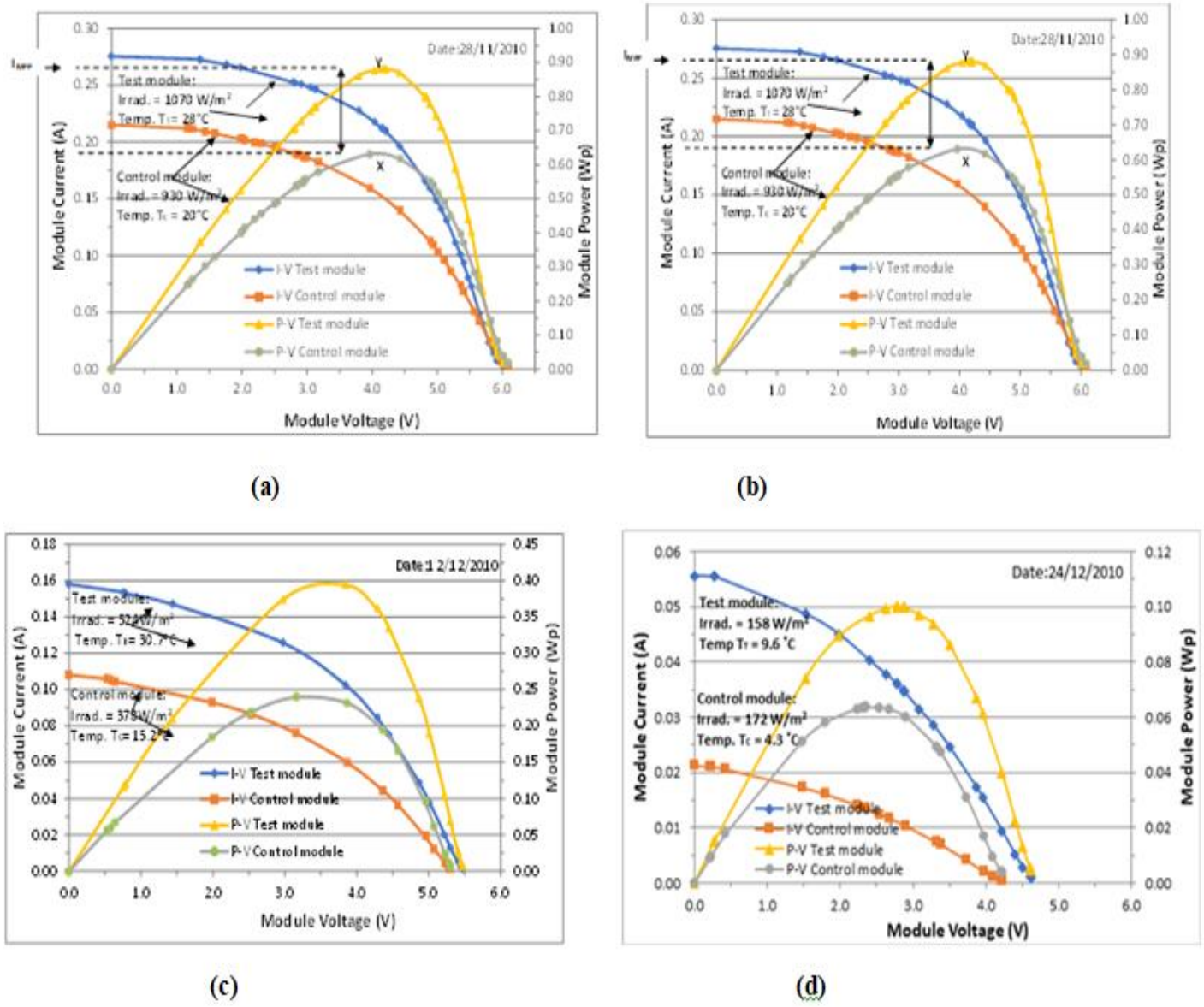

Fig. 6. I-V and P-V plots for test and control modules for (a) high insolation, (b) medium insolation, (c) low insolation, and (d) very low insolation.

The effect of the increased concentration on the open circuit voltage, V_{OC}, is evident in Figs. 6(a) - (c) and Figs. 7(a) – (b). The open circuit voltage was found to decrease slightly with a decrease in the insolation falling on it. At high insolation, where radiation intensity is greater than 900 W/m2, the open circuit voltage was approximately 6.2 V. Medium insolation days are days when the radiation intensity is between 650 and 850 W/m2 and it was found that the open circuit voltage is approximately 5.7 V. Increments ranging from 0.2 V to 0.5 V are common until the module is subjected to prolonged intensity, by which time VOC for the module subjected to concentration begins to decrease. During low insolation days, where radiation intensity is between 300 and 550 W/m^2, the open circuit voltage fell to between 5.4 and 5.5 V. On very low insolation days, where radiation intensity is less than 200 W/m^2, the open circuit voltage dropped to between 4.3 and 4.6 V.

2) *Power-voltage (P-V) characteristics: maximum power point*: The maximum power of a module or peak power (Watts-peak, Wp) is the output attained under standard test conditions of 1000 W/m^2 solar radiation at a module temperature of 25 ºC and air mass of 1.5. Air Mass is a quantity related to the depth or thickness of the atmosphere that affects the spectral composition of sunlight when the sun is at an altitude of 42º from the horizon [16] [18]. To get the most out of a module, it is necessary to operate it at the maximum power point where maximum power can be delivered to a load.

ISSN No. 2454-6194 | DOI: 10.51584/IJRIAS |Volume X Issue VI June 2025

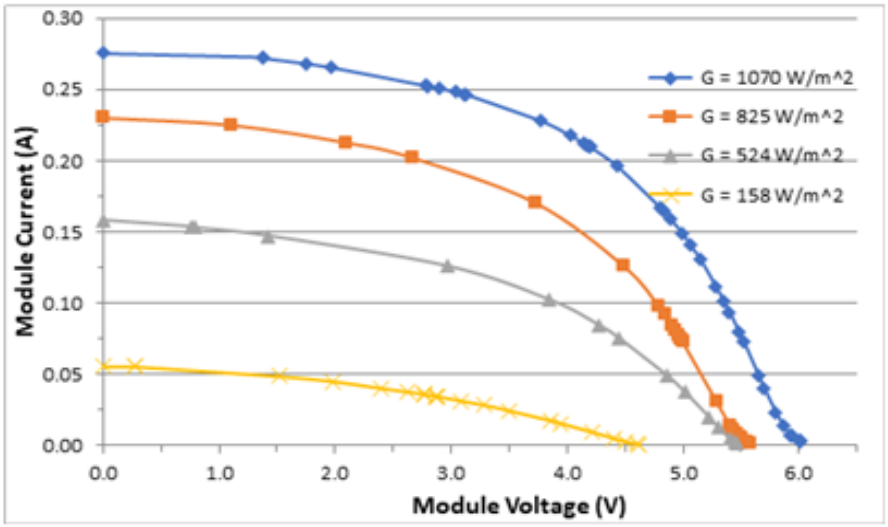

(a)

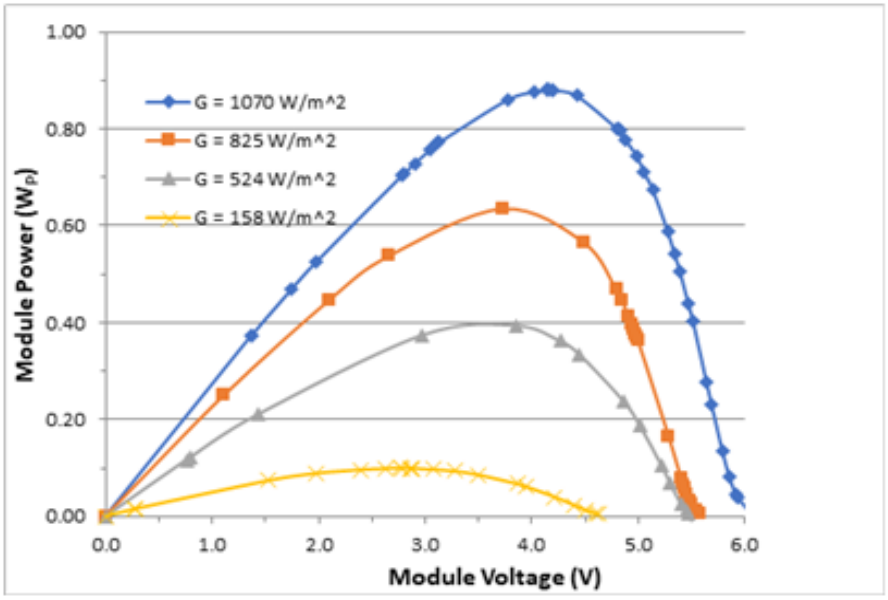

(b)

Fig. 7 (a) I-V characteristics and (b) P-V characteristics of the test module for various irradiances

Each of the P-V curves in Figs. 6 and 7(b) shows a marginal increase in maximum power point when the module is subjected to increased radiation from the Fresnel lens. P-V characteristics for the test module for different light intensity levels are depicted in Fig. 7 (b). The power yield of the test module is seen to increase with light intensity. As illustrated in Fig. 7 (b), the maximum power point increased from 0.631 Wp to 0.936 Wp. In Fig. 6 (a), points X and Y are respectively the maximum power points for the control and test modules. For increased irradiation from 930 W/m2 to 1070 W/m^2, a corresponding increase of 0.64 Wp to 0.88 Wp (an increase of about 38%) in maximum power was exhibited by the test module. Generally, power and hence energy yield increased with an increase in light intensity, particularly on medium to high insolation days. Electrical output currents and power as illustrated in Figs. 7 (a) and (b) respectively, show a progressive increase in direct proportion to a corresponding level of light intensity.

B. Variation of Current at Maximum Power with Irradiation

The variation of current at maximum power point versus irradiation is shown in Fig. 8. The photocurrent at a level ***X*** of irradiation (i.e., *G*) as a function of the photocurrent at 1 sun (1000 W/m^2) is expressed as [18]:

$$I_{PH} = X * I_{PH,(1\text{-}SUN)} \qquad (1)$$

ISSN No. 2454-6194 | DOI: 10.51584/IJRIAS |Volume X Issue VI June 2025

Since I_{MPP} is directly related to I_{PH}, a best line of fit was superimposed on the values obtained for each module to obtain a linear relationship between I_{MPP} and irradiation G. An equation relating the two variables shows the dependence of I_{MPP} on irradiation, thus validating the theory. From Eqn. 1, the equations of the straight lines in Fig. 8 can be expressed as:

Test module: $I_{MPP} = 0.0002G + 0.0033$ (2)

Control module: $I_{MPP} = 0.0002G - 0.0066$ (3)

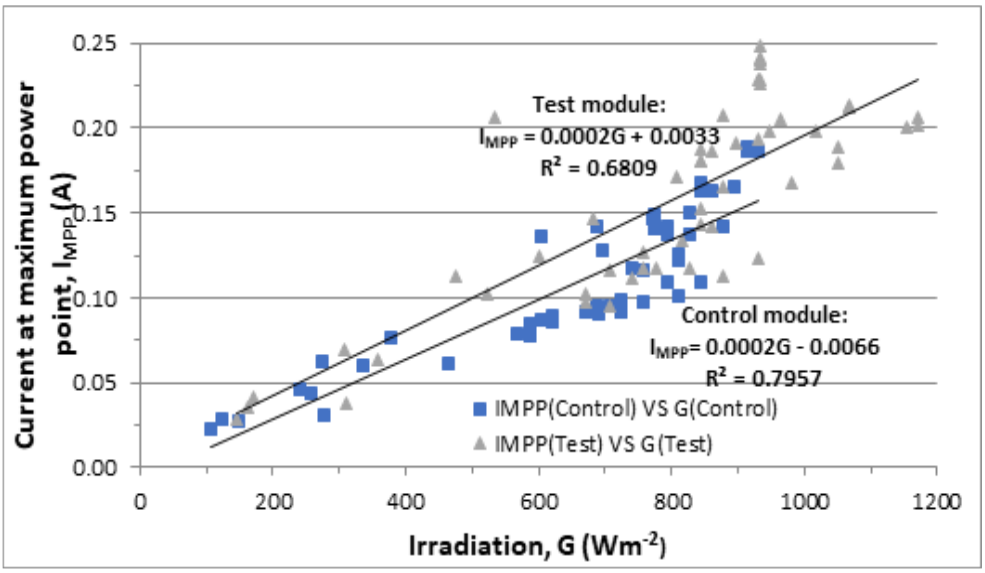

Fig. 8 Variation of current at maximum power point with irradiation, G.

Both lines can be seen to have identical slopes of 0.0002. The intercept on the control module shows a negative value, while that of the test module is a positive value, indicating an increment in IMPP, hence an increment in IPH due to increased concentration.

C. Variation of Maximum Power Point with Irradiation

A power curve was fitted to the respective sets of data points as illustrated in Fig. 9. Trend lines drawn through the points are also displayed.

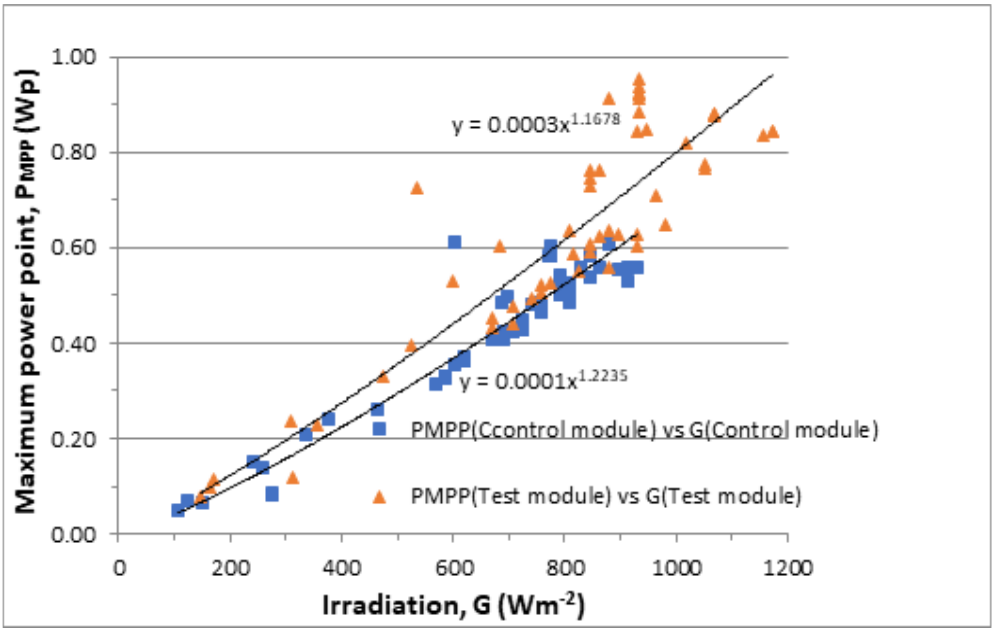

Fig. 9 Variation of maximum power point, PMPP, with irradiation, G.

ISSN No. 2454-6194 | DOI: 10.51584/IJRIAS |Volume X Issue VI June 2025

The equations obtained are as follows:

Test module: $P_{MPP} = 0.0003G^{1.1678}$ (4)

Control module: $P_{MPP} = 0.0001G^{1.2235}$ (5)

The respective residual sum of squares between observed and predicted values are:

Test module: RSS = 0.165

Control module: RSS = 0.155

The RSS values computed indicate the control module displays a better agreement to the equation than the test module by a margin of 0.01.

D. Effect of Temperature Increase

The solar intensity and ambient air temperature are two major determinants of the operating temperature of a solar PV [5]. Solar energy concentration is accountable for a significant increase in solar heat flux in the PV module. Figure 10 shows the outcome of increased temperature on both modules on 12 December 2010. The effects of increased temperature on the I-V and P-V curves are illustrated in Figs. 10(a) and (b), respectively. A change in short current ΔI_{SC} of 0.042 A was observed, which translated to a 22% increase while for the open circuit voltage, Voc = 5.578V was noted for the test module, and V_{OC} = 5.685 for the control, a decrement of ΔV_{OC} = -0.11V or approximately 2% drop in V_{OC}. The V_{OC} axis on the power curve for the test module was found to have fallen by a difference of about 0.15 V after a sustained temperature of 40 ˚C. Being winter period, with slight wind blowing, temperatures did not go higher than this on the test module.

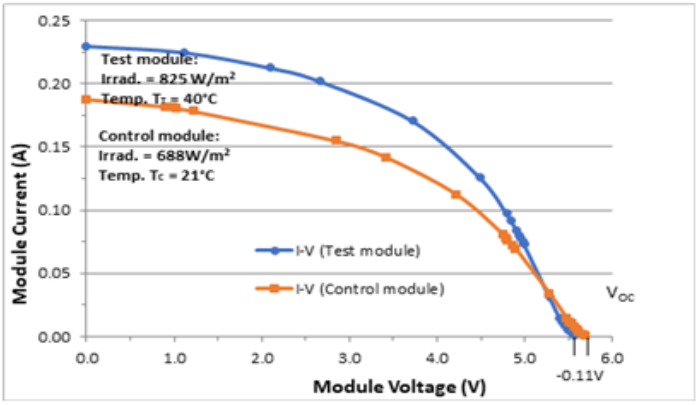

(a)

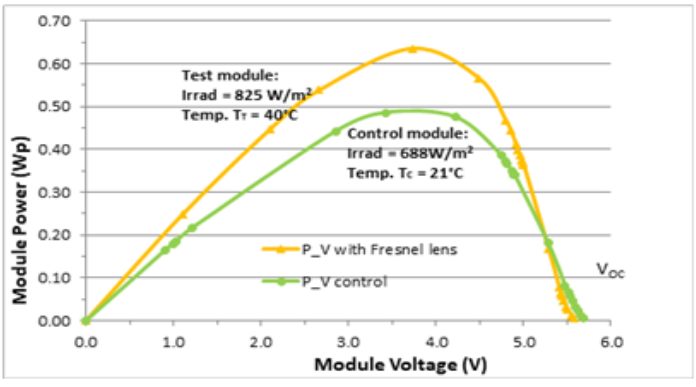

(b)

Fig. 10 Effect of increased temperature due to Fresnel lens on (a) I-V curves (b) P-V curves for 12 December 2010.

ISSN No. 2454-6194 | DOI: 10.51584/IJRIAS |Volume X Issue VI June 2025

In Fig. 11, the temperature and corresponding open circuit voltage on each panel were monitored on 28 November 2010 from about 1030 hrs to 1300 hrs. As the temperature of the test panel continued to rise, at some point, a little before 1100 hrs, the open circuit voltage of the test module dropped to below that of the control module and continued dropping until the test panel temperature was allowed to go up to 44 ˚C. An average difference of -0.11V was deduced between the open circuit voltages.

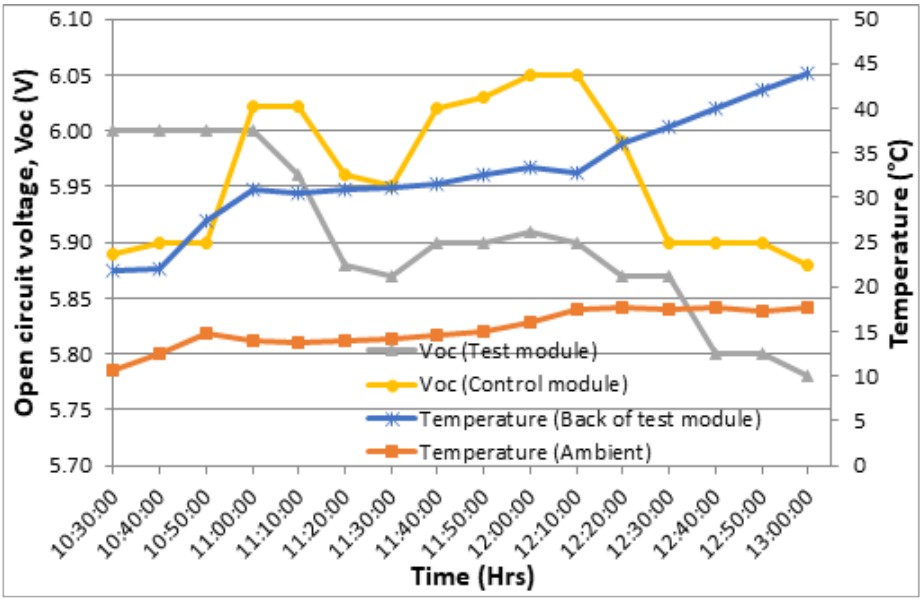

Fig. 11. Variation of open circuit voltage, Voc (V) with temperature for 28 November 2010.

E. Module Quality – Fill Factor, FF

A comparison of fill factors obtained at different times for the two modules is presented in Fig. 12. There was a general increase in fill factor values obtained for the test module compared to those of the control module, an indication of increased efficiency, albeit not substantial. A higher average *FF* of 0.487 was calculated for the test module while 0.45 was obtained for the control module. An average increase of 0.04 was computed for the days presented in the graph, i.e., an 8.2% increase. The effect of temperature on FF was observed not to be significant as the module was not subject to sustained or excessively high temperature.

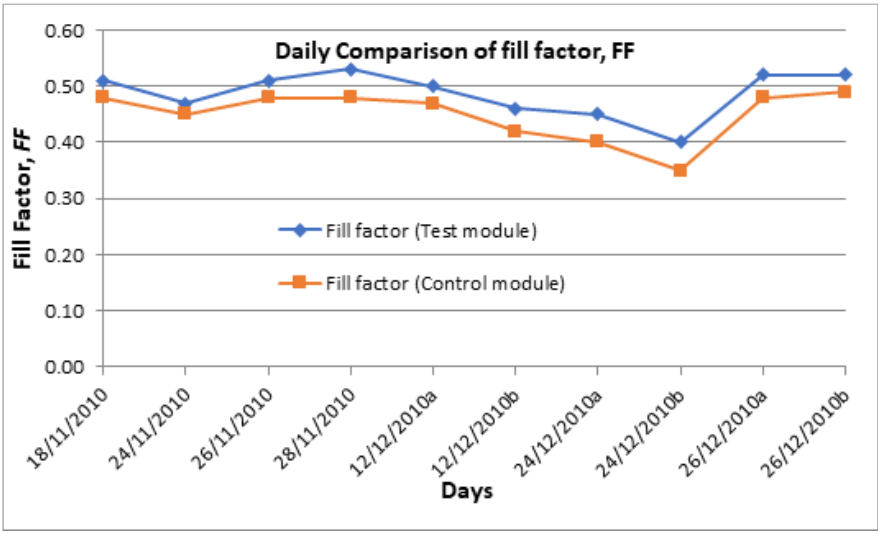

Fig. 12 Comparison of fill factor obtained for test and control modules

CONCLUSION

A non-conventional, low-concentration PV system with a Fresnel lens has been implemented to boost the power output of the PV module. The short circuit current and the maximum power output of the test module

ISSN No. 2454-6194 | DOI: 10.51584/IJRIAS |Volume X Issue VI June 2025

receiving concentrated solar radiation from the Fresnel lens were higher than those of the control module facing the sun directly for different levels of insolation ranging from ~158 W/m^2 to ~1070 W/m^2. An average increase of over 41% in the short circuit current was delivered by the test module in comparison to the control module. At maximum power points, the test module produced an average of about 52% more power than the control module. Generally, an improvement in energy yield was observed in the test module. Current at maximum power point increased linearly with increased radiation. A linear relationship was deduced between both parameters. The modelled data showed good agreement with observed data. An average increase of 53% was recorded for a percentage increase in maximum power point on the test module. A prolonged increase in temperature due to the increased irradiation caused the V_{OC} to diminish as expected but not too significantly. At a sustained temperature of 44 ˚C, a drop of nearly 0.5 V was noted on the test module. A general increase of over 8 % in fill factor values obtained for the test module compared to those of the control module, indicating increased efficiency. Some of the possible applications of the proposed system include rapid battery charging and other functional applications where twice as much energy is required in a short time. Apart from the monocrystalline silicon module considered in this study, the performance of polycrystalline and thin film amorphous silicon panels, which require low solar irradiation, can be evaluated in further studies. Unlike crystalline Si, amorphous silicon does not exhibit a pronounced decrease in nominal power due to increased temperature.

REFERENCES

1. Z. Sen, “Solar energy in progress and future trends,” Progress on energy and combustion science, vol. 30, pp. 367-416, 2004.
2. G. Boyle, Renewable energy, power for a sustainable future, 2nd ed., Oxford: Oxford University Press, 2004.
3. E. Alsema, M. de Wild-Scholten and V. Fthenakis, “Environmental impacts of PV generation – a critical comparison of energy supply options,” in 21st European Photovoltaic Solar Energy Conference, Dresden, Germany, 2006.
4. M. Brazilian, F. Leenders, B. Van Der Ree and D. Prasad, “Photovoltaic cogeneration in the built environment,” Solar energy, vol. 71, no. 1, pp. 57-69, 2001.
5. S. Wenham, M. Green, M. Watt and R. Corkish, Applied Photovoltaics, 2nd ed., Earthscan publishing, 2009.
6. F. Dincer and M. Meral, “Critical factors that affect the efficiency of solar cells. 1, pp.47-50. Smart grid and renewable energy, pp. 47-50, 2010.
7. N. Yang, Q. Liu, L. Xing, G. Wang, W. Zhang and J. Xuan, “A novel linear fresnel solar CPV/T hybrid system with advanced film beam splitter for optimal energy harvesting: Optical and thermodynamic analysis,” Energy, vol. 316, pp. 134460, 2025.
8. N. Patanasemakul, P. Rakkwamsuk and S. Chuangchote, “A comparative experimental investigation of CPV with and without SOE,” International Journal of Green Energy, 2019.
9. P. Boito and R. Grena, “Application of a fixed-receiver Linear Fresnel Reflector in concentrating photovoltaics,” Solar energy, vol. 215, pp. 198-205, 2021.
10. R. Hmouda, Y. Muzychka and X. Duan, “Experimental and Theoretical Modelling of Concentrating Photovoltaic Thermal System with Ge-Based Multi-Junction Solar Cells,” Energies, vol. 15, p. 4056, 2022.
11. H. Qiu, H. Liu, Q. Xia, Z. Lin and C. Chen, “A spectral splitting CPV/T hybrid system based on wave-selecting filter coated compound parabolic concentrator and linear Fresnel reflector concentrator,” Renewable Energy, vol. 226, p. 120403, 2024.
12. X. Kong, L. Zhang, H. Li, Y. Wang and M. Fan, “Experimental thermal and electrical performance analysis of a concentrating photovoltaic/thermal system integrated with phase change material (PV/T-CPCM),” Solar Energy Materials and Solar Cells, vol. 234, p. 111415, 2022.
13. M. Alzahrani, R. A. K. Shanks, S. Sundaram and T. Mallick, “Graphene as a pre-illumination cooling approach for a concentrator photovoltaic (CPV) system,” Solar Energy Materials & Solar Cells, vol. 222, p. 110922, 2021.

14. L. Guiqiang, Y. Lu, Q. Xuan, Y. Akhlaghi, G. Pei and J. Ji, "Small scale optimization in crystalline silicon solar cell on efficiency enhancement of low-concentrating photovoltaic cell," Solar Energy, vol. 202, pp. 316-325, 2020.
15. K. Rabah, "Integrated solar energy systems for rural electrification in Kenya," Renewable Energy., vol. 30, pp. 23-42, 2005.
16. H. Mousazadeh, A. Keyhani, A. Javadi, H. Mobli, K. Abrinia and A. Sharifi, "A review of principle and sun-tracking methods for maximizing solar systems output," Renewable and Sustainable Energy Reviews, vol. 13, pp. 1800-1818, 2009.
17. J. Parsons and S. Jha, "Using a Solar Concentrator with Photovoltaic Cells," 2009.
18. E. van Dyk, E. Meyer, F. Vorster and A. Leitch, "Long-term monitoring of photovoltaic devices," Renewable Energy, vol. 25, pp. 183-197, 2002.

APPENDIX

Appendix

1: PV Module Datasheet

Module Type: SA 1.5-12 Monocrystalline 12 cell

Dimensions without frame: 130mm x 130mm. **Area = 0.0169m^2**

Electrical data (at STC: 1000 W/m^2, AM1.5, and a cell temperature of 25^{o}C).

Rated power	P_{max}	1.5Wp
Rated voltage	$Vmpp$	6V
Rated current	$Impp$	0.25A
Open circuit voltage	V_{OC}	7.1V
Short circuit current	I_{SC}	0.278A
Cell efficiency		14.5%

The current, voltage and power temperature coefficients were not supplied for the modules.